

Amorphous Ultrathin SnO₂ Films by Atomic Layer Deposition on Graphene Network as Highly Stable Anodes for Lithium-Ion Batteries

Ming Xie,[†] Xiang Sun,[‡] Steven M. George,[§] Changgong Zhou,[⊥] Jie Lian,^{*,‡} and Yun Zhou^{*,¶}

[†]Wuhan ATMK Super EnerG Technologies, Inc., #7-5 JiaYuan Road, Wuhan 430073, China

[‡]Department of Mechanical, Aerospace, and Nuclear Engineering, Rensselaer Polytechnic Institute, 110 Eighth Street, Troy, New York 12180, United States

[§]Department of Chemistry and Biochemistry and Department of Mechanical Engineering, University of Colorado at Boulder, Boulder, Colorado 80309, United States

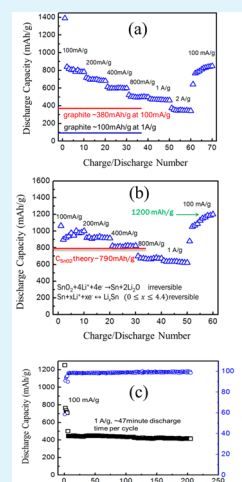
[⊥]Natural Science Department, Lawrence Technological University, Southfield, Michigan 48075, United States

[¶]College of Chemistry, Chongqing Normal University, Chongqing 401311, China

Supporting Information

ABSTRACT: Amorphous SnO₂ (a-SnO₂) thin films were conformally coated onto the surface of reduced graphene oxide (G) using atomic layer deposition (ALD). The electrochemical characteristics of the a-SnO₂/G nanocomposites were then determined using cyclic voltammetry and galvanostatic charge/discharge curves. Because the SnO₂ ALD films were ultrathin and amorphous, the impact of the large volume expansion of SnO₂ upon cycling was greatly reduced. With as few as five formation cycles best reported in the literature, a-SnO₂/G nanocomposites reached stable capacities of 800 mAh g⁻¹ at 100 mA g⁻¹ and 450 mAh g⁻¹ at 1000 mA g⁻¹. The capacity from a-SnO₂ is higher than the bulk theoretical values. The extra capacity is attributed to additional interfacial charge storage resulting from the high surface area of the a-SnO₂/G nanocomposites. These results demonstrate that metal oxide ALD on high surface area conducting carbon substrates can be used to fabricate high power and high capacity electrode materials for lithium-ion batteries.

KEYWORDS: atomic layer deposition, critical size, conformal, amorphous SnO₂, interfacial capacity

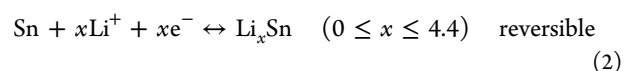
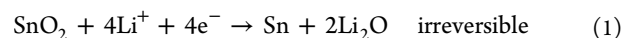


INTRODUCTION

The development of portable electronic devices and hybrid electric cars requires advanced lithium-ion batteries (LIBs) with large energy densities, fast rate capabilities, prolonged lifetime, and low cost. However, the current commercial graphite anode has a low gravimetric capacity of 372 mAh g⁻¹, which leads to a limited energy output density of LIBs.¹ Transition metal oxides with higher theoretical capacities (>600 mAh g⁻¹) have been exploited as alternative anode materials including Fe₃O₄/Fe₂O₃,^{2–4} Co₃O₄/CoO,^{5–8} Mn₃O₄,⁹ NiO,¹⁰ MoO₃/MoO₂,^{11,12} and CuO.¹³ Si, Sn, Ge, and Al form alloys with Li and are also being considered. Among them, Sn-based material is the only commercialized anode in the market. However, Co has to be added as 1:1 ratio into composites to reach satisfying performance.¹⁴ To prevent using expensive Co, SnO₂ has become an alternative anode and attracted much attention these years.^{15–17}

The reaction of Li with SnO₂ consists of two steps. The first step is irreversible and produces Li₂O and Sn, then a series of

tin–lithium alloys forms in the second step (reactions 1 and 2):¹⁸



A series of Li–Sn alloys (Li₂Sn₅, LiSn, Li₇Sn₃, Li₅Sn₂, Li₁₃Sn₅, Li₇Sn₂, and Li₂₂Sn₅) are formed between 0 and 0.6 V versus Li/Li⁺.¹⁹ The highest theoretical capacity for Li–Sn alloy can reach 782 mAh g⁻¹ (Li₂₂Sn₅). However, it also brings a 250% volume change,²⁰ which results in electrode pulverization and eventually capacity fading.^{19,21} The common strategy is to grow SnO₂ nanoparticles on surface of carbonaceous substrates, such as graphene and carbon nanotubes, or design novel nanostructured SnO₂. Although these routines can greatly improve performance of SnO₂, it usually requires the 15–30

Received: September 15, 2015

Accepted: November 25, 2015

Published: November 25, 2015

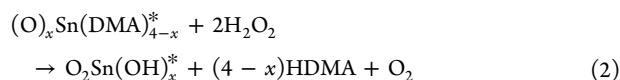
cycles to reach stable capacities.^{16,22–38} This is because large SnO₂ nanostructure breaks down into its critical size (~3 nm)²² and eventually form a stable solid–electrolyte interphase (SEI). This process continuously consumes precious lithium from the cathode, which causes a deteriorated performance in a full cell. Although the initial coulombic efficiency (CE) can be improved by adding surface-stabilized lithium metal powders,²³ it cannot provide enough lithium reservoir for a long formation process without sacrificing safety and energy density. Therefore, if SnO₂ should to be considered as an alternative to the commercial graphite anode, it is critical to reduce formation cycles down to several cycles, ideally, one cycle.

Atomic layer deposition (ALD) is an important thin film growth technique that utilizes sequential self-limiting surface reactions to deposit ultrathin films with Ångstrom-level control.²⁴ In addition, the chemical reactions in ALD form strong covalent linkages between the ALD film and the underlying substrate. This covalent linkage can significantly enhance the stability of the deposited metal oxide ALD films. ALD can precisely control the size, morphology, and crystallinity of films or nanoparticles than wet chemical methods such as sol–gel, hydrothermal, and electroplating processing.^{25–27} Therefore, ALD is an ideal tool to deposit SnO₂ nanostructure under its critical size and with desired morphology.

In this work, we reported the synthesis of aSnO₂ thin film uniformly along surfaces of graphene network by ALD. The two-dimensional sheet structure of graphene provides an excellent building block to tolerant volume change during charge/discharge. Compared to the previously reported ALD SnO₂/G anode,²⁸ a different Sn precursor and deposition process were chosen, which gave much improved cycling performance. Within five formation cycles, SnO₂/G anode reached its stability. In addition, we also discussed the extra capacity contributed from grain boundary and the effect of crystallinity on cycling stability.

EXPERIMENTAL DETAILS

Graphene sheets were produced by thermal exfoliation of the as-synthesized GO powders.²⁹ Details of the graphene synthesis can be found in our previous publications.^{30,31} SnO₂ ALD was grown directly on graphene powders using a rotary ALD reactor.^{32,33} Specifically, tetrakis(dimethylamino) tin (TDMASn, Gelest, > 95% purity) and high-performance liquid chromatography (HPLC) grade water (H₂O, Aldrich) were used in this work. The TDMASn was held in a stainless steel bubbler maintained at 65 °C. SnO₂ ALD was performed at 150 °C using alternating TDMASn and H₂O exposures in an ABAB... sequence:



where the asterisks represent the surface species. The typical growth rate for the SnO₂ ALD chemistry is ~0.6 Å per cycle,³⁴ and thus the thickness of SnO₂ film can be well controlled at the nanometer scale by ALD cycles. The SnO₂ ALD reaction sequence was: (i) TDMASn dose to 1.0 Torr; (ii) evacuation of reaction products and excess TDMASn with N₂ purging; (iii) H₂O dose to 1.0 Torr; and (iv) evacuation of reaction products and excess H₂O with N₂ purging.

The phase, crystallinity, and microstructure of the ALD SnO₂ were characterized by X-ray diffraction (XRD) using PAN analytical X-ray diffraction system, scanning electron microscopy (SEM) by a Carl Zeiss Ultra 1540 Dual Beam FIB/SEM System, and a transmission

electron microscopy (TEM) using a JEOL JEM-2010 instrument, operated at 200 kV. X-ray photoelectron spectroscopy (XPS) was performed using a PHI 5000 Versa Probe system. The surface area and pore size distribution were measured using a Quantachrome AUTOSORB-1 instrument, with the samples heated at 150 °C under vacuum for 12 h before testing. Thermogravimetric analysis (TGA) was performed in air from 30–700 °C at a heating rate of 10 °C/min in a TA Instrument TGA-Q50.

The electrodes were made by mixing SnO₂/G nanocomposites with polyvinylidene fluoride (PVDF) and carbon black at a weight ratio of 75:15:10 in 1-methyl-2-pyrrolidinone solvent. The slurry was coated on copper foil by blade and dried under vacuum at 80 °C overnight. All of the cells were assembled in an argon-filled drybox with Li metal as the negative electrode. A Celgard separator 2340 and 1 M LiPF₆ electrolyte solution in 1:1 w/w ethylene carbonate and diethyl carbonate (Novolyte) were used to fabricate the coin cells. Cyclic voltammetry (CV) measurement was carried out using a potentiostat VersaSTAT 4 (Princeton Applied Research) at a scan rate of 0.5 mV s⁻¹. Galvanostatic charge/discharge cycles were performed at a voltage range of 3–0.01 V using an Arbin BT 2000 testing station. The mass loading of SnO₂/G nanocomposites is ~1–2 mg/cm².

RESULTS AND DISCUSSION

Graphene nanosheets were prepared by thermal exfoliation of graphite oxide, and therefore defects and residual oxygen functional groups inevitably existed in the structure of graphene. These defective sites serve as the initial nucleation sites for the controllable growth of SnO₂ by ALD. However, the difficulty of the total removal water from high surface area may cause a little CVD growth, leading to thin film growth instead of particles. The large distribution of mesoporous structure developed upon thermal exfoliation³¹ allows the gas phase ALD precursors to diffuse into the internal structures of G, which results in uniform SnO₂ film along surface of 3-D graphene matrix.

As observed from SEM analysis (Figure 1), the SnO₂ film is uniformly anchored along the porous network of wrinkled

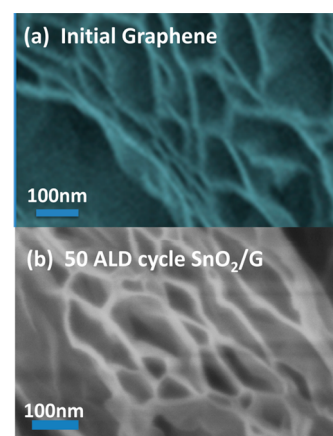


Figure 1. SEM of pristine G and 50 cycle ALD SnO₂/G composites.

graphene. No SnO₂ particles can be seen. The highly dense coverage of surface defects (carboxyl or hydroxyl groups) on graphene allows the uniform surface interaction with ALD precursors. The high-resolution TEM image (not shown) did not observe any nanoparticles and crystalline structures. It is very difficult to distinguish amorphous SnO₂ film from graphene sheets due to lack of lattice contrast. The graphene sheets synthesized by graphite oxidization followed by thermal exfoliation and reduction were evaluated using Raman

spectroscopy. The D- and G-bands of graphene and the prominent D-band ($\sim 1350\text{ cm}^{-1}$) to G-band ($\sim 1580\text{ cm}^{-1}$) ratio reveal that there are structure disorders and defects caused by the extensive oxidation in making graphite oxides.^{35,36} A more detailed study can be found in our previous work.³⁷

TGA measurement as shown in Figure S1 in Supporting Information indicates that the mass percentage of SnO_2 in the composites reaches 53% for 50 ALD cycles. The high mass loading of active material is critical to realize the feasibility of using ALD for large-scale nanocomposite powder production. Here, we adapted static dosing ALD precursors instead of flow-type ALD since static dosing can reach much higher reactant utilization efficiency and allow coating high surface area substrates such as graphene and CNTs powder.³² Our results indicate that more than 50 wt % of active materials can be achieved with less than 50 ALD cycles. The greatly reduced ALD deposition time and cost, along with maximized precursor utilization efficiency, make ALD possible for large-scale powder production. At this time, we have the capability of synthesizing nanocomposites in a batch quantity of 10 g of powder per ALD run at a lab scale.

The nitrogen adsorption/desorption isotherms of SnO_2/G composites together with the pore size distribution, derived based on the density functional theory (DFT) model, are shown in Figure S2. The sample displays the typical type IV isotherm with a large hysteresis loop, demonstrating that the significant amount of mesopores, which initially existed in the graphene,³¹ were preserved after ALD deposition. The broad pore distributions from 3–35 nm almost remain intact after deposition, resulting from the unique self-limiting reaction of ALD. Such open structure is expected to provide easy access of electrolytes and facilitate the fast Li-ion diffusion when used as a potential LIB material. The specific surface area is $240\text{ m}^2/\text{g}$ for 50 ALD cycles SnO_2/G composites, compared to $450\text{ m}^2/\text{g}$ for pristine graphene. The reduced surface area is a result of the overall reduction in specific area with increased mass loading of SnO_2 . Figure 2, panel a shows the XPS spectrum of the SnO_2/G composites, which reveals the presence of carbon, oxygen, and tin. The Sn 3d regions with two peaks centered at 494.9 and 486.5 eV (Figure 2b) indicate the existence of Sn (IV). These XPS results verify the presence of SnO_2 on graphene.

Electrodes made with the SnO_2/G nanocomposites were tested in coin cells with lithium metal as a counter electrode. Cyclic voltammograms of SnO_2/G nanocomposites were measured between 0.01 and 3 V at a scan rate of 0.5 mV/s. Figure S3 shows the first and fifth cycle of CV of SnO_2/G nanocomposite electrode. In the first cycle, the first two reduction peaks at ~ 1.2 and 0.8 V are observed and can be ascribed to the reduction of SnO_2 to Sn^{38} and formation of SEI.³⁹ The peaks around 0.5 V and below are assigned to the formation of Li–Sn alloy. The broad peak at ~ 0.5 V is an overlap of delithiation reaction of LiSn alloy.⁴⁰ The high current response near 0 V indicates the lithium intercalation into the graphene backbone.^{5,8} In the subsequent anodic scans, the peak at ~ 0.6 V corresponds to a series of dealloying of LiSn. The peak at ~ 1.2 V is believed to be due to lithium extraction from carbon.²⁶ There are also some literatures ascribing this peak to reform SnO_2 from Sn and Li_2O .⁴¹ The CV curves also show good reproducibility in the fifth cycle, suggesting a high reversibility of the lithium and SnO_2 reaction.

Figure 3 presents the voltage profiles of SnO_2/G composites for the first five cycles at a current density of 100 mA g^{-1} . The initial discharge capacity is 1250 mAh g^{-1} due to formation of

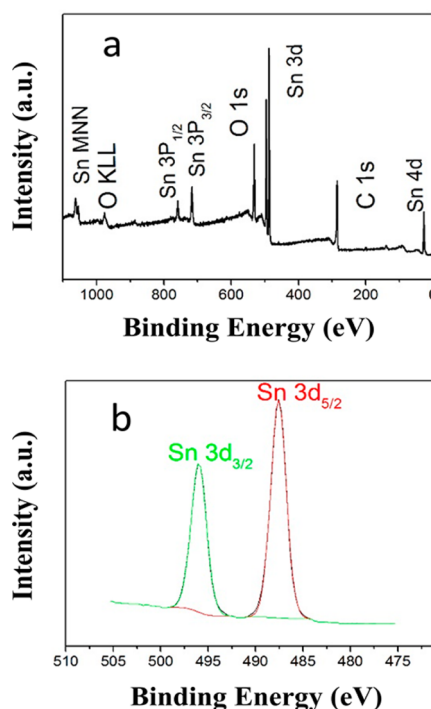


Figure 2. (a) XPS spectrum of the SnO_2/G composites (b) Sn 3d XPS spectra.

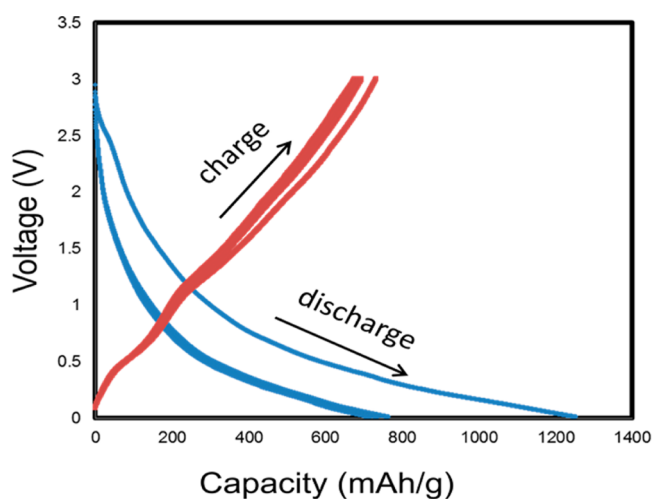


Figure 3. Galvanostatic charge/discharge curves at current density of 100 mA/g for the first five cycles.

SEI and Li_2O . The charge capacity is 730 mAh g^{-1} , corresponding to an initial coulombic efficiency of $\sim 60\%$. From the second cycle, the discharge curves are almost overlapped. No obvious plateau was seen during discharging, but two voltage plateaus at ~ 0.6 and 1.2 V were observed from the charging curves, consistent with CV analysis.

Excellent rate performance has been achieved using 50 ALD cycle SnO_2/G nanocomposites, as shown in Figure 4, panel a, at various current densities. The cell has been continuously cycled without any rest between different rates. A high capacity $\sim 800\text{ mAh g}^{-1}$ is obtained at 100 mA g^{-1} . SnO_2/G nanocomposites are able to maintain $\sim 500\text{ mAh g}^{-1}$ capacity even when the current density is increased to 1000 mA g^{-1} , retaining $\sim 63\%$ of its discharge capacity at 100 mA g^{-1} . This is much higher than the capacity of graphite, which can only

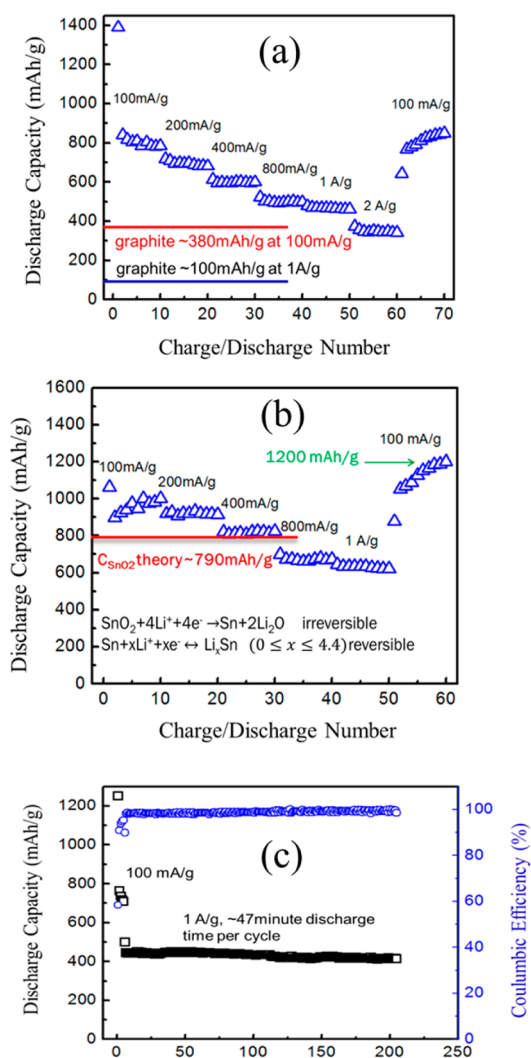


Figure 4. (a) Rate performance of SnO₂/G composites at various current densities; (b) rate performance of SnO₂ contribution only at various current densities; (c) cycling performance and CE of SnO₂/G composites at 1000 mA g⁻¹.

preserve ~30% of its original capacity at a rate of ~1000 mA g⁻¹.⁴² The specific capacity of a-SnO₂ is calculated by subtracting the graphene contributions from the nanocomposites shown in Figure 4, panel b. The actual contribution of the graphene in the evaluation of the SnO₂ ALD-coated graphene electrodes could be even lower because the graphene is completely covered with SnO₂ ALD films.

We also studied the long-term stability of SnO₂/G at fast charge/discharge rates. Figure 4, panel c shows the cycling performance of SnO₂/G at 1 A g⁻¹. The first five cycles were stabilized at 100 mA g⁻¹ to ensure the enough activation and formation of stable SEI.⁴³ After 200 cycles, the capacity retention was ~92%, and SnO₂/G can still deliver a reversible capacity of 410 mAh g⁻¹ and maintain the CE over 99.5%. We would like to point out that at ~110 cycles, the sudden capacity drop is caused by a power outage. After the process resumed, the capacity shows no decay until the 200th cycle. Therefore, we believe the actual capacity retention should be higher than 92%. We attribute the good rate performance to the synergistic effect of amorphous thin film morphology of SnO₂ and

conductive 3-D graphene matrix, which ensure fast lithium-ion diffusion and electron transfer.

The excellent electrochemical performance of SnO₂/G nanocomposites can be attributed to several potential factors: (1) ALD allows for the deposition of SnO₂ film under the critical size below which the pulverization of large SnO₂ nanoparticles (250% volume expansion/contraction during discharge/charge processes) can be greatly mitigated; (2) ultrathin SnO₂ film shortens the Li⁺ diffusion path, resulting in a very impressive rate performance; (3) the 3-D structure of SnO₂/G nanocomposites greatly enhances lithium diffusion and electron conduction; (4) the excellent mechanical properties of graphene can accommodate the large volume change of SnO₂; and (5) the chemical bonding between SnO₂ and graphene prevents the aggregation of nanoparticles during cycling.

Five formation cycles for Sn-based anodes are comparable to the commercial graphite and to our best knowledge, is the best reported in the literature summarized in Table 1. The short formation cycle is critical for SnO₂-based anode in a full cell. The common cause for long formation cycles is due to SEI formation and lack of stable electrode structure. When the anode's volume changes during charge/discharge, the fresh surface is continuously exposed to the electrolyte, which causes irreversible loss until the structure reaches equilibrium and a stable SEI is formed. ALD can ensure film and nanoparticles under their critical size (~3 nm) so the volume expansion is much less dramatic compared to larger particles size reported by other techniques. In addition, carbonaceous materials with large surface areas tends to form significant amount of SEI at the defects and edge plane.⁴⁴ For example, graphene's oxygen-containing surface functional groups are very reactive and can oxidize the electrolyte and consequently induce electrochemical instability in the electrode. For wet-chemistry based synthesis, SnO₂ is prone to nucleate on those defect sites and edge plane as well; however, it is impossible to completely cover them. In contrast, because of its separated gas phase reaction, those sites can easily attract ALD precursors and form complete coverage on defects and edge, reducing the irreversible loss and formation cycles

SnO₂ ALD for lithium anode was previously reported by using SnCl₄ and H₂O as precursors.²⁸ It has the highest capacity of 793 mAh g⁻¹ at 400 mA g⁻¹. However, its capacity decreases until the 10th cycle and then keeps increasing for 200 cycles. No stable capacity can be observed. We believe this is probably due to the different ALD chemistry. Our group has shown that SnCl₄ and H₂O form very low quality of SnO₂ films at 200 °C with a high percentage of Cl residue.⁴⁵ The Cl residue may further form LiCl with Li⁺, which causes irreversible lithium loss and long formation cycles. In addition, a thicker film had to be formed to cover the surface of graphene conformally in that literature.²⁸ The gradually increased capacity phenomenon was also observed in many other literatures. However, we believe this phenomenon may cause more concerns than its benefits. A full cell consists of a pair of matched cathode and anode, which should provide the same energy (Ah). To prevent lithium plating and improve the safety, the anode has to be carefully calculated to accommodate lithium provided by the cathode. The gradually increased capacity makes it impossible to use in a battery, although some amazing capacities are reported. If any other material is considered as an alternative to graphite anode, a stable capacity should be reached within several cycles, ideally less than five

Table 1. Comparison of Different SnO₂ Anode Reported in Literature with This Work

materials	highest capacity	formation cycle number	initial Coulombic efficiency	reference
SnO ₂ /graphene	840 mAh g ⁻¹ at 67 mA g ⁻¹	~15	58%	55
SnO ₂ /graphene	635 mAh g ⁻¹ at 60 mA g ⁻¹	~30	44%	56
SnO ₂ /ferrocene-encapsulated SWCNT	905 mAh g ⁻¹ at 150 mA g ⁻¹	~15	60%	57
SnO ₂ /graphene	570 mAh g ⁻¹ at 50 mA g ⁻¹	~30	43%	16
SnO ₂ /N-doped graphene	1346 mAh g ⁻¹ at 500 mA g ⁻¹	capacity decreases for ~25 cycles and then increases until 500 cycles	61.3%	58
nano-Sn/C	710 mAh g ⁻¹ at 200 mA g ⁻¹	~20	69%	40
SnO ₂ /G	718 mAh g ⁻¹ at 100 mA g ⁻¹	~25	68%	59
SnO ₂ /MWCNT	420 mAh g ⁻¹ at 156 mA g ⁻¹	~60	56%	60
Sn-core/carbon-sheath nanocable	630 mAh g ⁻¹ at 100 mA g ⁻¹	~50	66.9%	61
interconnected SnO ₂ nanoparticles	778 mAh g ⁻¹ at 78 mA g ⁻¹	~20	50%	62
ultrasmall SnO ₂ particles in micro/mesoporous carbon	560 mAh g ⁻¹ at 1400 mA g ⁻¹	~30	44%	63
Sn anchored on graphene	1022 mAh g ⁻¹ at 200 mA g ⁻¹	~100	69%	64
owl-like SnO ₂ @carbon hollow particles	1282 mAh g ⁻¹ at 100 mA g ⁻¹	~15	68.4%	65
SnO ₂ nanowires coated with ALD TiO ₂	883 mAh g ⁻¹ at 400 mA g ⁻¹	~50	67.7%	66
SnO ₂ /G with ALD HfO ₂	853 mAh g ⁻¹ at 150 mA g ⁻¹	~40	61.7%	67
SnO ₂ /graphene by ALD	793 mAh g ⁻¹ at 400 mA g ⁻¹	capacity decreases for ~10 cycles, increases for 200 cycles, and decreases until 400 cycles	49.5%	28
SnO ₂ /graphene by ALD	800 mAh g ⁻¹ at 100 mA g ⁻¹	~5; stable for at least 200 cycles	60%	this work

cycles. Therefore, people would know how much anode they should use to match with the cathode. Another critical parameter is the initial CE. Higher than 80% of the initial CE is usually required, preferably higher than 85%. None of literatures listed in Table 1 reaches this requirement. We have tried to use Al₂O₃ ALD and alucone MLD on silicon anode and achieved 85% of CE (unpublished). We believe the same strategy can be applied to SnO₂/G anode and will be further studied in the future.

Another important issue studied in this work is where the high capacity of SnO₂ comes. So far, there are two possible explanations: (1) reversible reaction from Sn to SnO₂, which gives a total theoretical capacity of 1494 mAh g⁻¹; or (2) interfacial storage at grain boundaries. The evidence for the first explanation is the peak at ~1.2 V from CV analysis.⁴¹ However, there is a strong argument against this hypothesis that metallic Sn/carbon composites also have the same peak.^{25,26} To further understand the possible source for this extra capacity, we intentionally created oxygen vacancy to form SnO_x, which consists of SnO₂, SnO, and Sn. If the first step is indeed reversible, then decreasing oxygen content will reduce the contribution from the first reaction step to the total capacity. We expect SnO_x to have lower capacity than SnO₂ if the first step is reversible. In this experiment, we annealed as-grown SnO₂/G nanocomposite in H₂ atmosphere at 300 and 400 °C for 2 h. XRD in Figure 5 shows that as-grown SnO₂/G has amorphous structure. After annealing 300 °C in H₂, SnO₂ peaks become more profound, indicating an improved crystalline structure. A slight weight loss was also observed due to oxygen

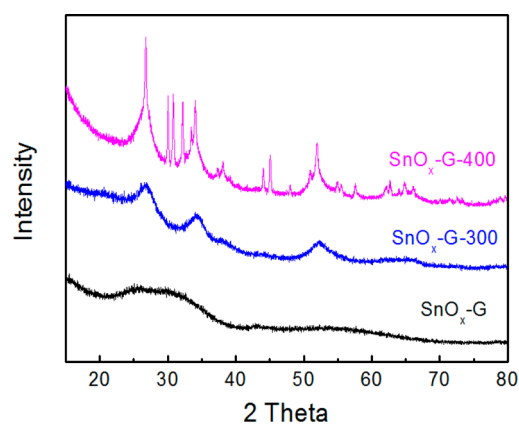


Figure 5. XRD of SnO₂/G nanocomposite and after H₂ annealing at 300 and 400 °C.

loss. After 400 °C annealing with H₂, SnO₂/G became a mixture of SnO₂, SnO and metallic Sn.⁴⁶ We tested their rate performances using the same conditions as amorphous SnO₂/G in Figure 6. The capacities of annealed samples were almost overlapped with amorphous SnO₂/G, but with a slightly degraded cycling stability. This result indicates the total capacity from SnO₂ is independent of its oxygen content. Therefore, the first reaction step should not be reversible. We believe that the extra capacity from our system is probably due to interfacial storage. Maier et al. describe a phenomenon upon which lithium ions collect at grain boundaries, which results in

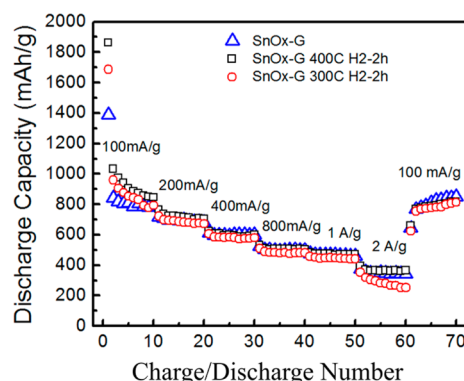


Figure 6. Rate performance of SnO₂/G composites as grown, SnO₂/G composites annealed with H₂ at 300 °C for 2 h, and SnO₂/G composites annealed with H₂ at 400 °C for 2 h at various current densities.

both battery and capacitor-like properties.^{47–49} There have been quite a few studies of SnO₂ for supercapacitors.^{50,51} A high capacity of 363 F g⁻¹ was reported for SnO₂ smaller than 10 nm recently.⁵² However, to achieve reversible interfacial storage, a system must have stable grain boundaries in spite of the large volume change. This can only be realized with nanoparticle/film under its critical size and with minimal volume change. In addition, amorphous structure shows better capacity retention due to its isotropic volume expansion compared to directional volume expansion of crystalline structure. This is consistent with conclusions from the literature.^{28,53,54}

CONCLUSION

We have successfully synthesized SnO₂ thin film along the surface of graphene by ALD. ALD allows depositing SnO₂ under its critical size with controlled morphology and crystallinity, which give exceptional electrochemical performance. Fifty ALD cycles of SnO₂/G exhibit a stable capacity of 800 mAh g⁻¹ at 100 mA g⁻¹ and 450 mAh g⁻¹ at 1000 mA g⁻¹. By subtracting the graphene contribution from the composites, SnO₂ displays an unprecedented specific capacity of 1200 mAh g⁻¹, higher than the theoretical capacity. The long cycling test under 1000 mA g⁻¹ shows a very stable lifetime and nearly 100% CE. More importantly, SnO₂/G nanocomposites show much shorter formation cycles compared to nanostructured SnO₂ synthesized by other techniques. To our best knowledge, our SnO₂/G nanocomposites reach the stable capacity with the least formation cycles reported in the literature. We believe that fewer formation cycles are more critical to realize Sn-based anodes than simply attempting high capacity and rate performance. H₂ annealing test indicates the extra capacity from SnO₂ is probably due to interfacial storage instead of reformation of SnO₂ from Sn and Li₂O. The ALD process represents an innovative approach to synthesize advanced metal oxide-based electrodes for stable and high-performance LIBs.

ASSOCIATED CONTENT

Supporting Information

The Supporting Information is available free of charge on the ACS Publications website at DOI: 10.1021/acsami.5b08719.

Figure of TGA of ALD SnO₂/G composites; figure of Nitrogen adsorption/desorption isotherms of SnO₂/G composites and DFT pore size distribution; figure of CV

curves of 50 ALD cycle SnO₂/G composite at the first and fifth cycle (PDF)

AUTHOR INFORMATION

Corresponding Authors

*E-mail: yunzhou@cqu.edu.cn.

*E-mail: lianj@rpi.edu.

Notes

The authors declare no competing financial interest.

ACKNOWLEDGMENTS

The work at Chongqing Normal University was supported by the Natural Science Foundation of China (No. 21301199), Chongqing Municipal Education Commission (KJ130601), and Natural Science Foundation of Chongqing Municipality (cstc2014jcyjA50035). This work at Rensselaer Polytechnic Institute was supported by a NSF Career Award under the Award No. DMR 1151028. This work at Wuhan ATKM Super EnerG Technologies Inc. was supported by the 3551 Recruitment Program of Global Experts by Wuhan East Lake Hi-Tech Development Zone, China. The work at the University of Colorado was supported by the Defense Advanced Research Project Agency (DARPA).

REFERENCES

- (1) Tarascon, J. M.; Armand, M. Issues and Challenges Facing Rechargeable Lithium Batteries. *Nature* **2001**, *414* (6861), 359–367.
- (2) Zhou, G. M.; Wang, D. W.; Li, F.; Zhang, L. L.; Li, N.; Wu, Z. S.; Wen, L.; Lu, G. Q.; Cheng, H. M. Graphene-Wrapped Fe₃O₄ Anode Material with Improved Reversible Capacity and Cyclic Stability for Lithium Ion Batteries. *Chem. Mater.* **2010**, *22* (18), 5306–5313.
- (3) Ji, L. W.; Tan, Z. K.; Kuykendall, T. R.; Aloni, S.; Xun, S. D.; Lin, E.; Battaglia, V.; Zhang, Y. G. Fe₃O₄ Nanoparticle-Integrated Graphene Sheets for High-Performance Half and Full Lithium Ion Cells. *Phys. Chem. Chem. Phys.* **2011**, *13* (15), 7139–7146.
- (4) Zhu, X. J.; Zhu, Y. W.; Murali, S.; Stoller, M. D.; Ruoff, R. S. Nanostructured Reduced Graphene Oxide/Fe₂O₃ Composite As a High-Performance Anode Material for Lithium Ion Batteries. *ACS Nano* **2011**, *5* (4), 3333–3338.
- (5) Wu, Z. S.; Ren, W. C.; Wen, L.; Gao, L. B.; Zhao, J. P.; Chen, Z. P.; Zhou, G. M.; Li, F.; Cheng, H. M. Graphene Anchored with Co₃O₄ Nanoparticles as Anode of Lithium Ion Batteries with Enhanced Reversible Capacity and Cyclic Performance. *ACS Nano* **2010**, *4* (6), 3187–3194.
- (6) Li, B. J.; Cao, H. Q.; Shao, J.; Li, G. Q.; Qu, M. Z.; Yin, G. Co₃O₄@graphene Composites as Anode Materials for High-Performance Lithium Ion Batteries. *Inorg. Chem.* **2011**, *50* (5), 1628–1632.
- (7) Kim, H.; Seo, D. H.; Kim, S. W.; Kim, J.; Kang, K. Highly Reversible Co₃O₄/Graphene Hybrid Anode for Lithium Rechargeable Batteries. *Carbon* **2011**, *49* (1), 326–332.
- (8) Peng, C. X.; Chen, B. D.; Qin, Y.; Yang, S. H.; Li, C. Z.; Zuo, Y. H.; Liu, S. Y.; Yang, J. H. Facile Ultrasonic Synthesis of CoO Quantum Dot/Graphene Nanosheet Composites with High Lithium Storage Capacity. *ACS Nano* **2012**, *6* (2), 1074–1081.
- (9) Wang, H. L.; Cui, L. F.; Yang, Y. A.; Sanchez Casalongue, H.; Robinson, J. T.; Liang, Y. Y.; Cui, Y.; Dai, H. J. Mn₃O₄-Graphene Hybrid as a High-Capacity Anode Material for Lithium Ion Batteries. *J. Am. Chem. Soc.* **2010**, *132* (40), 13978–13980.
- (10) Zou, Y. Q.; Wang, Y. NiO Nanosheets Grown on Graphene Nanosheets as Superior Anode Materials for Li-ion Batteries. *Nanoscale* **2011**, *3* (6), 2615–2620.
- (11) Xu, Y.; Yi, R.; Yuan, B.; Wu, X. F.; Dunwell, M.; Lin, Q. L.; Fei, L.; Deng, S. G.; Andersen, P.; Wang, D. H.; Luo, H. M. High Capacity MoO₃/Graphite Oxide Composite Anode for Lithium-Ion Batteries. *J. Phys. Chem. Lett.* **2012**, *3* (3), 309–314.

- (12) Tao, T.; Glushenkov, A. M.; Zhang, C. F.; Zhang, H. Z.; Zhou, D.; Guo, Z. P.; Liu, H. K.; Chen, Q. Y.; Hu, H. P.; Chen, Y. MoO₃ Nanoparticles Dispersed Uniformly in Carbon Matrix: a High Capacity Composite Anode for Li-ion Batteries. *J. Mater. Chem.* **2011**, *21* (25), 9350–9355.
- (13) Wang, B.; Wu, X. L.; Shu, C. Y.; Guo, Y. G.; Wang, C. R. Synthesis of CuO/Graphene Nanocomposite as a High-Performance Anode Material for Lithium-ion Batteries. *J. Mater. Chem.* **2010**, *20* (47), 10661–10664.
- (14) Whittingham, M. S. Materials Challenges Facing Electrical Energy Storage. *MRS Bull.* **2008**, *33* (4), 411–419.
- (15) Wang, D. H.; Kou, R.; Choi, D.; Yang, Z. G.; Nie, Z. M.; Li, J.; Saraf, L. V.; Hu, D. H.; Zhang, J. G.; Graff, G. L.; Liu, J.; Pope, M. A.; Aksay, I. A. Ternary Self-Assembly of Ordered Metal Oxide-Graphene Nanocomposites for Electrochemical Energy Storage. *ACS Nano* **2010**, *4* (3), 1587–1595.
- (16) Paek, S. M.; Yoo, E.; Honma, I. Enhanced Cyclic Performance and Lithium Storage Capacity of SnO₂/Graphene Nanoporous Electrodes with Three-Dimensionally Delaminated Flexible Structure. *Nano Lett.* **2009**, *9* (1), 72–75.
- (17) Zhang, L. S.; Jiang, L. Y.; Yan, H. J.; Wang, W. D.; Wang, W.; Song, W. G.; Guo, Y. G.; Wan, L. J. Mono Dispersed SnO₂ Nanoparticles on Both Sides of Single Layer Graphene Sheets as Anode Materials in Li-ion Batteries. *J. Mater. Chem.* **2010**, *20* (26), 5462–5467.
- (18) Courtney, I. A.; Dahn, J. R. Key Factors Controlling the Reversibility of the Reaction of Lithium with SnO₂ and Sn₂BP₆O₆ Glass. *J. Electrochem. Soc.* **1997**, *144* (9), 2943–2948.
- (19) Winter, M.; Besenhard, J. O. Electrochemical Lithiation of Tin and Tin-Based Intermetallics and Composites. *Electrochim. Acta* **1999**, *45* (1–2), 31–50.
- (20) Besenhard, J. O.; Winter, M. Advances in Battery Technology: Rechargeable Magnesium Batteries and Novel Negative-Electrode Materials for Lithium Ion Batteries. *ChemPhysChem* **2002**, *3* (2), 155–159.
- (21) Besenhard, J. O.; Yang, J.; Winter, M. Will Advanced Lithium-Alloy Anodes Have a Chance in Lithium-Ion Batteries? *J. Power Sources* **1997**, *68* (1), 87–90.
- (22) Kim, C.; Noh, M.; Choi, M.; Cho, J.; Park, B. Critical Size of a Nano SnO₂ Electrode for Li-Secondary Battery. *Chem. Mater.* **2005**, *17* (12), 3297–3301.
- (23) Forney, M. W.; Ganter, M. J.; Staub, J. W.; Ridgley, R. D.; Landi, B. J. Prelithiation of Silicon-Carbon Nanotube Anodes for Lithium Ion Batteries by Stabilized Lithium Metal Powder (SLMP). *Nano Lett.* **2013**, *13* (9), 4158–4163.
- (24) Jung, Y. S.; Cavanagh, A. S.; Dillon, A. C.; Groner, M. D.; George, S. M.; Lee, S.-H. Enhanced Stability of LiCoO₂ Cathodes in Lithium-Ion Batteries Using Surface Modification by Atomic Layer Deposition. *J. Electrochem. Soc.* **2010**, *157* (1), A75–A81.
- (25) Liu, J. H.; Chen, J. S.; Wei, X. F.; Lou, X. W.; Liu, X. W. Sandwich-Like, Stacked Ultrathin Titanate Nanosheets for Ultrafast Lithium Storage. *Adv. Mater.* **2011**, *23* (8), 998–1002.
- (26) Wang, D. H.; Choi, D. W.; Li, J.; Yang, Z. G.; Nie, Z. M.; Kou, R.; Hu, D. H.; Wang, C. M.; Saraf, L. V.; Zhang, J. G.; Aksay, I. A.; Liu, J. Self-Assembled TiO(2)-Graphene Hybrid Nanostructures for Enhanced Li-Ion Insertion. *ACS Nano* **2009**, *3* (4), 907–914.
- (27) Li, N.; Liu, G.; Zhen, C.; Li, F.; Zhang, L. L.; Cheng, H. M. Battery Performance and Photocatalytic Activity of Mesoporous Anatase TiO₂ Nanospheres/Graphene Composites by Template-Free Self-Assembly. *Adv. Funct. Mater.* **2011**, *21* (9), 1717–1722.
- (28) Li, X. F.; Meng, X. B.; Liu, J.; Geng, D. S.; Zhang, Y.; Banis, M. N.; Li, Y. L.; Yang, J. L.; Li, R. Y.; Sun, X. L.; Cai, M.; Verbrugge, M. W. Tin Oxide with Controlled Morphology and Crystallinity by Atomic Layer Deposition onto Graphene Nanosheets for Enhanced Lithium Storage. *Adv. Funct. Mater.* **2012**, *22* (8), 1647–1654.
- (29) McAllister, M. J.; Li, J. L.; Adamson, D. H.; Schniepp, H. C.; Abdala, A. A.; Liu, J.; Herrera-Alonso, M.; Milius, D. L.; Car, R.; Prud'homme, R. K.; Aksay, I. A. Single Sheet Functionalized Graphene by Oxidation and Thermal Expansion of Graphite. *Chem. Mater.* **2007**, *19* (18), 4396–4404.
- (30) Wang, G. K.; Sun, X.; Lu, F. Y.; Yu, Q. K.; Liu, C. S.; Lian, J. Controlled Synthesis of MnSn(OH)(6)/Graphene Nanocomposites and Their Electrochemical Properties as Capacitive Materials. *J. Solid State Chem.* **2012**, *185*, 172–179.
- (31) Sun, X.; Xie, M.; Wang, G. K.; Sun, H. T.; Cavanagh, A. S.; Travis, J. J.; George, S. M.; Lian, J. Atomic Layer Deposition of TiO₂ on Graphene for Supercapacitors. *J. Electrochem. Soc.* **2012**, *159* (4), A364–A369.
- (32) McCormick, J. A.; Cloutier, B. L.; Weimer, A. W.; George, S. M. Rotary Reactor for Atomic Layer Deposition on Large Quantities of Nanoparticles. *J. Vac. Sci. Technol., A* **2007**, *25* (1), 67–74.
- (33) Cavanagh, A. S.; Wilson, C. A.; Weimer, A. W.; George, S. M. Atomic Layer Deposition on Gram Quantities of Multi-Walled Carbon Nanotubes. *Nanotechnology* **2009**, *20* (25), 255602.
- (34) Elam, J. W.; Baker, D. A.; Hryn, A. J.; Martinson, A. B. F.; Pellin, M. J.; Hupp, J. T. Atomic Layer Deposition of Tin Oxide Films Using Tetrakis(dimethylamino) Tin. *J. Vac. Sci. Technol., A* **2008**, *26* (2), 244–252.
- (35) Obratsov, A. N.; Tyurnina, A. V.; Obratsova, E. A.; Zolotukhin, A. A.; Liu, B. H.; Chin, K. C.; Wee, A. T. S. Raman Scattering Characterization of CVD Graphite Films. *Carbon* **2008**, *46* (6), 963–968.
- (36) Stankovich, S.; Dikin, D. A.; Piner, R. D.; Kohlhaas, K. A.; Kleinhammes, A.; Jia, Y.; Wu, Y.; Nguyen, S. T.; Ruoff, R. S. Synthesis of Graphene-Based Nanosheets Via Chemical Reduction of Exfoliated Graphite Oxide. *Carbon* **2007**, *45* (7), 1558–1565.
- (37) Ban, C. M.; Xie, M.; Sun, X.; Travis, J. J.; Wang, G. K.; Sun, H. T.; Dillon, A. C.; Lian, J.; George, S. M. Atomic Layer Deposition of Amorphous TiO₂ on Graphene as an Anode for Li-Ion Batteries. *Nanotechnology* **2013**, *24* (42), 424002.
- (38) Lin, Y. M.; Nagarale, R. K.; Klavetter, K. C.; Heller, A.; Mullins, C. B. SnO₂ and TiO₂-Supported-SnO₂ Lithium Battery Anodes with Improved Electrochemical Performance. *J. Mater. Chem.* **2012**, *22* (22), 11134–11139.
- (39) Huang, X. H.; Xia, X. H.; Yuan, Y. F.; Zhou, F. Porous ZnO Nanosheets Grown on Copper Substrates as Anodes for Lithium Ion Batteries. *Electrochim. Acta* **2011**, *56* (14), 4960–4965.
- (40) Xu, Y. H.; Liu, Q.; Zhu, Y. J.; Liu, Y. H.; Langrock, A.; Zachariah, M. R.; Wang, C. S. Uniform Nano-Sn/C Composite Anodes for Lithium Ion Batteries. *Nano Lett.* **2013**, *13* (2), 470–474.
- (41) Xu, W.; Canfield, N. L.; Wang, D. Y.; Xiao, J.; Nie, Z. M.; Zhang, J. G. A Three-Dimensional Macroporous Cu/SnO₂ Composite Anode Sheet Prepared via a Novel Method. *J. Power Sources* **2010**, *195* (21), 7403–7408.
- (42) Sivakkumar, S. R.; Nerkar, J. Y.; Pandolfo, A. G. Rate Capability of Graphite Materials as Negative Electrodes in Lithium-Ion Capacitors. *Electrochim. Acta* **2010**, *55* (9), 3330–3335.
- (43) Chaudhari, S.; Srinivasan, M. 1D Hollow Alpha-Fe₂O₃ Electrospun Nanofibers as High Performance Anode Material for Lithium Ion Batteries. *J. Mater. Chem.* **2012**, *22* (43), 23049–23056.
- (44) Pumera, M. Graphene-Based Nanomaterials for Energy Storage. *Energy Environ. Sci.* **2011**, *4* (3), 668–674.
- (45) Du, X.; Du, Y.; George, S. M. In Situ Examination of Tin Oxide Atomic Layer Deposition Using Quartz Crystal Microbalance and Fourier Transform Infrared Techniques. *J. Vac. Sci. Technol., A* **2005**, *23* (4), 581–588.
- (46) Wu, P.; Du, N.; Zhang, H.; Yu, J. X.; Qi, Y.; Yang, D. R. Carbon-Coated SnO₂ Nanotubes: Template-Engaged Synthesis and Their Application in Lithium-Ion Batteries. *Nanoscale* **2011**, *3* (2), 746–750.
- (47) Jamnik, J.; Maier, J. Nanocrystallinity Effects in Lithium Battery Materials - Aspects of Nano-Ionics. Part IV. *Phys. Chem. Chem. Phys.* **2003**, *5* (23), 5215–5220.
- (48) Maier, J. Mass Storage in Space Charge Regions of Nano-Sized Systems (Nano-Ionics. Part V). *Faraday Discuss.* **2007**, *134*, 51–66.
- (49) Maier, J. Nanoionics: Ionic Charge Carriers in Small Systems. *Phys. Chem. Chem. Phys.* **2009**, *11* (17), 3011–3022.

- (50) Rakhi, R. B.; Chen, W.; Cha, D. K.; Alshareef, H. N. High Performance Supercapacitors Using Metal Oxide Anchored Graphene Nanosheet Electrodes. *J. Mater. Chem.* **2011**, *21* (40), 16197–16204.
- (51) Liu, P.; Tang, B. J.; Zhao, J. C.; Feng, J. C.; Xu, J. L. Ordered Mesoporous Carbon/SnO₂ Composites as the Electrode Material for Supercapacitors. *J. Wuhan Univ. Technol., Mater. Sci. Ed.* **2011**, *26* (3), 407–411.
- (52) Lim, S. P.; Huang, N. M.; Lim, H. N. Solvothermal Synthesis of SnO₂/Graphene Nanocomposites for Supercapacitor Application. *Ceram. Int.* **2013**, *39* (6), 6647–6655.
- (53) Mohamedi, M.; Lee, S. J.; Takahashi, D.; Nishizawa, M.; Itoh, T.; Uchida, I. Amorphous Tin Oxide Films: Preparation and Characterization as an Anode Active Material for Lithium Ion Batteries. *Electrochim. Acta* **2001**, *46* (8), 1161–1168.
- (54) Sun, X.; Zhou, C. G.; Xie, M.; Hu, T.; Sun, H. T.; Xin, G. Q.; Wang, G. K.; George, S. M.; Lian, J. Amorphous Vanadium Oxide Coating on Graphene by Atomic Layer Deposition for Stable High Energy Lithium Ion Anodes. *Chem. Commun.* **2014**, *50* (73), 10703–10706.
- (55) Wang, X. Y.; Zhou, X. F.; Yao, K.; Zhang, J. G.; Liu, Z. P. A SnO₂/Graphene Composite as a High Stability Electrode for Lithium Ion Batteries. *Carbon* **2011**, *49* (1), 133–139.
- (56) Wang, D. N.; Li, X. F.; Wang, J. J.; Yang, J. L.; Geng, D. S.; Li, R. Y.; Cai, M.; Sham, T. K.; Sun, X. L. Defect-Rich Crystalline SnO₂ Immobilized on Graphene Nanosheets with Enhanced Cycle Performance for Li Ion Batteries. *J. Phys. Chem. C* **2012**, *116* (42), 22149–22156.
- (57) Li, J. X.; Zhao, Y.; Wang, N.; Guan, L. H. A High Performance Carrier for SnO₂ Nanoparticles Used in Lithium Ion Battery. *Chem. Commun.* **2011**, *47* (18), 5238–5240.
- (58) Wen, Z. H.; Cui, S. M.; Kim, H. J.; Mao, S.; Yu, K. H.; Lu, G. H.; Pu, H. H.; Mao, O.; Chen, J. H. Binding Sn-Based Nanoparticles on Graphene as the Anode of Rechargeable Lithium-Ion Batteries. *J. Mater. Chem.* **2012**, *22* (8), 3300–3306.
- (59) Wang, L.; Wang, D.; Dong, Z. H.; Zhang, F. X.; Jin, J. Interface Chemistry Engineering for Stable Cycling of Reduced GO/SnO₂ Nanocomposites for Lithium Ion Battery. *Nano Lett.* **2013**, *13* (4), 1711–1716.
- (60) Jin, Y. H.; Min, K. M.; Seo, S. D.; Shim, H. W.; Kim, D. W. Enhanced Li Storage Capacity in 3 nm Diameter SnO₂ Nanocrystals Firmly Anchored on Multiwalled Carbon Nanotubes. *J. Phys. Chem. C* **2011**, *115* (44), 22062–22067.
- (61) Luo, B.; Wang, B.; Liang, M. H.; Ning, J.; Li, X. L.; Zhi, L. J. Reduced Graphene Oxide-Mediated Growth of Uniform Tin-Core/Carbon-Sheath Coaxial Nanocables with Enhanced Lithium Ion Storage Properties. *Adv. Mater.* **2012**, *24* (11), 1405–1409.
- (62) Etacheri, V.; Seisenbaeva, G. A.; Caruthers, J.; Daniel, G.; Nedelec, J.-M.; Kessler, V. G.; Pol, V. G. Ordered Network of Interconnected SnO₂ Nanoparticles for Excellent Lithium-Ion Storage. *Adv. Energy Mater.* **2015**, *5*. DOI: [10.1002/aenm.201401289](https://doi.org/10.1002/aenm.201401289).
- (63) Jahel, A.; Ghimbeu, C. M.; Monconduit, L.; Vix-Guterl, C. Confined Ultrasmall SnO₂ Particles in Micro/Mesoporous Carbon as an Extremely Long Cycle-Life Anode Material for Li-Ion Batteries. *Adv. Energy Mater.* **2014**, *4* (11). DOI: [10.1002/aenm.201400025](https://doi.org/10.1002/aenm.201400025).
- (64) Qin, J.; He, C. N.; Zhao, N. Q.; Wang, Z. Y.; Shi, C. S.; Liu, E. Z.; Li, J. J. Graphene Networks Anchored with Sn@Graphene as Lithium Ion Battery Anode. *ACS Nano* **2014**, *8* (2), 1728–1738.
- (65) Liang, J.; Yu, X.-Y.; Zhou, H.; Wu, H. B.; Ding, S.; Lou, X. W. Bowl-like SnO₂@Carbon Hollow Particles as an Advanced Anode Material for Lithium-Ion Batteries. *Angew. Chem., Int. Ed.* **2014**, *53* (47), 12803–12807.
- (66) Guan, C.; Wang, X. H.; Zhang, Q.; Fan, Z. X.; Zhang, H.; Fan, H. J. Highly Stable and Reversible Lithium Storage in SnO₂ Nanowires Surface Coated with a Uniform Hollow Shell by Atomic Layer Deposition. *Nano Lett.* **2014**, *14* (8), 4852–4858.
- (67) Yesibolati, N.; Shahid, M.; Chen, W.; Hedhili, M. N.; Reuter, M. C.; Ross, F. M.; Alshareef, H. N. SnO₂ Anode Surface Passivation by Atomic Layer Deposited HfO₂ Improves Li-Ion Battery Performance. *Small* **2014**, *10* (14), 2849–2858.